# SIRT2 Promotes Murine Melanoma Progression Through Natural Killer Cell Inhibition

**Manchao Zhang**
University of Arkansas for Medical Sciences
**Scarlett Acklin**
University of Arkansas for Medical Sciences
**John Gillenwater**
University of Arkansas for Medical Sciences
**Wuying Du**
University of Arkansas for Medical Sciences
**Mousumi Patra**
University of Arkansas for Medical Sciences
**Hao Yu**
University of Arkansas for Medical Sciences
**Jianhua Yu**
City Of Hope National Medical Center
**Fen Xia** ( fxia@uams.edu )
University of Arkansas for Medical Sciences

**Research Article**

**Keywords:** SIRT2, melanoma models, tumor-infiltrating, oncogene, tumor suppressor

**Posted Date:** December 3rd, 2020

**DOI:** https://doi.org/10.21203/rs.3.rs-113402/v1

# Abstract

SIRT2, an $NAD^+$-dependent histone deacetylase, has been shown to play a pivotal role in various physiological processes, however, its role in cancer is currently controversial. In recent years, SIRT2 has been described as both a tumor suppressor and oncogene with divergent expression and function in various malignancies. Using murine xenograft melanoma models, our results suggest increased systemic expression of SIRT2 promotes tumor progression. In this study, SIRT2-overexpressing mice exhibited enhanced tumor growth and larger tumor volumes compared to their wild-type littermates. Mechanistically, systemic overexpression of SIRT2 reduces the number of tumor-infiltrating natural killer (NK) cells and suppresses NK cell activation and proliferation within the tumor microenvironment (TME). Furthermore, despite the effect of increased tumor growth rate and tumor volume in wild-type littermate mice, NK cell depletion does not affect that in SIRT2-overexpressing mice. Lastly, pharmacological inhibition of SIRT2 increases NK cell tumor infiltration and suppresses melanoma tumor growth in mice. The findings of this study identify a dynamic functional interaction between systemic SIRT2 and NK cell activity, which promotes melanoma tumor progression. Given the recent renewed interest in NK-cell-mediated immunotherapy response, SIRT2 could present a new opportunity to mediate immunotherapy response and resistance.


# Introduction

Described roles of SIRT2, a member of the sirtuin family of $NAD^+$-dependent deacetylases, have been extensive and diverse, but also conflicting. SIRT2 has been implicated in a myriad of physiological processes including metabolism [1], inflammation [2], aging [3], DNA repair [4], and cell cycle checkpoints [5]. It has also been shown to play a role in genomic stability and is integral to reducing tumor occurrence in liver and breast [6-9]. However, conflicting evidence characterizes SIRT2 as an integral component of GBM and melanoma proliferation and tumorigenicity [10,11]. With this study, we sought to further explore the complex relationship between SIRT2 and tumor progression.

SIRT2's established roles in inflammation and glucose and iron metabolism, all known regulators of tumor progression [7,12-15], indicate that systemic and microenvironment SIRT2, rather than just expression in tumor cells, might have implications on progression of tumors once they have already undergone tumorigenesis. The tumor microenvironment (TME), with effects on angiogenesis, immune response, and fibroblast growth factor, is an established major determinant of long-term tumor progression [16-18]. One such example is PTEN, a well-known tumor suppressor, that inhibits tumor cell growth in tumor cell, also suppresses breast tumor progression through stromal fibroblasts [19,20]. Moreover, the importance of the tumor immune microenvironment cannot be overstated, especially in the era of tumor immunotherapy. While much attention is focused on cytotoxic T lymphocytes, many other leukocytes play a role, particularly natural killer (NK) cells, which have increasingly been characterized as tumor suppressive mediators [7,17,21-24]. Interestingly, there is evidence supporting a connection between SIRT2 expression and NK cell function within the TME [14]. In murine hepatocellular carcinoma models, the microenvironments consistently promoted SIRT2 expression in NK cells, and exogenous

SIRT2 was successful in upregulating production of tumoricidal mediators[7]. SIRT2 has also been shown to increase Nrf2, an inducer of NK-cell-mediated tumor surveillance [25,26].

It is well understood that SIRT2 is involved in maintaining genomic stability in healthy cells [27], but there is lacking evidence for its definitive role in cancer initiation, tumor progression, and the TME. In this study, we examined SIRT2's effect on xenograft melanoma tumor progression using SIRT2 transgenic and wild-type mouse models, as well as underlying changes within the TME. We further demonstrated mice overexpressing SIRT2 show enhanced tumor progression as well as decreased NK cell infiltration and functional activity within the tumor. Altogether, our data demonstrate a novel role for systemic SIRT2 expression on NK cell function and tumor progression.

# Methods

*Cell lines and culture*

The B16-F10 *Mus musculus* skin melanoma cell line of C57BL/6 origin was obtained from Dr. Michael Ostrowski's laboratory at Ohio State University and was cultured in RPMI-1640 Medium (Gibco, USA) supplemented with 10% (v/v) fetal bovine serum (FBS) (Invitrogen, USA), 100 ug/mL penicillin, and 100 µg/mL streptomycin (Gibco, USA). All cells were maintained in a humidified environment with 5% (v/v) $CO_2$ at 37°C and were in the logarithmic growth phase when harvested for injection with ~50% confluence in B16-F10 cell line.

*B16-F10 cell Sirt2 knockout with CRISPR/Cas9 gene editing and Sirt2 overexpression*

Mouse SIRT2 CRISPR KO lentivirus vector targeting 5'- GTCATCTGTTTGGTGGGAGC-3' was purchased from Applied Biological Materials Inc. (Richmond, BC, Canada). Third generation lentivirus was packed as previously described[42]. B16-F10 cells were infected by lentivirus and selected in the medium containing 2.0 µg/ml puromycin to obtain stable B16-F10 *Sirt2*-KO cell line. B16-F10 cells were also transfected with Flag-tagged WT-*Sirt2* using FuGENE HD (Promega, Madison, WI) as before [42] to get SIRT2-overexpressing stable B16-F10 cell line after selection with 1,000 µg/ml neomycin.

*Animals*

$SIRT2^{+/+}$ (C57BL/6), *Sirt2* transgenic (*Sirt2*-KI or *SIRT2tg* [28]) and wild-type littermates with a C57BL/6 background were obtained from the Sinclair Laboratory (David A. Sinclair, PhD) in the Department of Genetics at Harvard Medical School. $SIRT2^{-/-}$ C57BL/6 (*Sirt2*-KO) mice were obtained from Tiago F. Outeiro (Department of Neurodegeneration and Restorative Research, Center for Nanoscale Microscopy and Molecular Physiology of the Brain, University Medical Center Göttingen). All mice were bred in the facilities of the Department of Laboratory Animal Medicine (DLAM) at the University of Arkansas for Medical Sciences. All procedures were approved by the University of Arkansas for Medical Sciences Institutional Animal Care and Use Committee (IACUC). All mouse experiments were performed in accordance with NIH regulations about the use and care of experimental animals. Appropriate numbers

of tumor cells were suspended in ice-cold phosphate-buffered saline (PBS) and checked for viability using trypan blue staining. Only when cell viability was greater than 90% was the cell batch considered for injection.

*Mouse subcutaneous melanoma xenograft model and treatment*

For the subcutaneous melanoma model, 6-8-week-old *Sirt2*-KI and wild-type littermates were inoculated subcutaneously with $1\times10^5$ B16-F10 melanoma cells resuspended in 100µl ice-cold PBS per injection into the lower flank. The day of tumor cell inoculation was designated as day 0. Measurement of tumor size began on the $6^{th}$ day and continued up to 20 days post injection. For each tumor measurement, the tumor's longest dimension (a) and the one perpendicular to it (b) were measured using digital caliper once every 2 to 3 days. Tumor volume (V) was calculated according to the following formula: $V = \pi/6 \times ab^2$. The volumes calculated with this formula were closely related to the weight of the tumors isolated after sacrifice (data not shown). For tumor treatment, SIRT2 was pharmacologically inhibited with the SIRT2 specific inhibitor, SirReal2 (Cat #S7845), ordered from Selleck Chemicals (Houston, TX, USA). It was dissolved in DMSO as an 84 mg/ml stock solution and stored at -20ºC. Daily vehicle or SirReal2 treatment (50 mg/kg in PBS containing 20% PEG400 and 10% Tween-20) was given 5 days before B16-F10 tumor inoculation and repeated once every 3 days until the end of the experiment.

*NK cell detection*

Mice tumor tissues were harvested from the tumor-bearing mice on days 14-15 after tumor transplantation. The tumor infiltrating lymphocytes (TIL) were isolated via Ficoll-Paque Premium (GE Healthcare, Pittsburgh, PA, USA) density gradient centrifugation after mincing in cell culture medium containing cell culture dish, grinding with a 5 ml syringe plunger on and passing through the 70 µm cell strainer. Next, $10^6$ TILs were pelleted, re-suspended in 50 µL blocking buffer (HBSS containing 5% normal mouse serum, 1:100 Fc blocker 24G.2 antibody, cat#553141, BD Biosciences, San Jose, CA), and incubated on ice for 30 min. Subsequently, the cells were re-suspended and incubated in the antibody cocktail containing 1:100-1:400 of anti-mouse CD45 (clone 30-F11, eBioscience, San Diego, CA, USA), CD19 (1D3), CD3e (145-2C11), NKp46 (29A1.4), and Fixable Viability Dye 780 (BD Biosciences) on ice for another 30 min protected from light. Finally, the cells were washed, fixed with 4% paraformaldehyde, washed again, passed through the 70-µm cell strainer lid of flow cytometry sample tubes in HBSS with 2% FBS. The samples were wrapped with aluminum foil and stored in 4°C refrigerator until flow cytometry analysis. For NK cell detection, the stained TIL samples were tested with LSRII flow cytometer (BD Biosciences), with live cells gated first, then $CD45^+$ cells, $CD19^-$cells from $CD45^+$ cells, $CD3e^-$cells from $CD45^+CD19^-$ cells, and $NKp46^+$ cells from $CD45^+CD19^-CD3e^-$ cells. Data analysis was performed via FlowJo software (Tree Star, Ashland, OR, USA).

*Depletion of NK cells in vivo*

To deplete the NK cells in subcutaneous melanoma bearing mice, the C57BL/6 and C57BL/6 *Sirt2*-KI mice were subcutaneously injected with B16-F10 cells on day 0 as described above. All mice in the NK-cell depletion groups were intraperitoneally injected with 50 mL of antibodies against Asialo-GM1 (AsGM1, Wako, Osaka, Japan) combined with 50 mL of distilled water before the injection of the tumor cells and then once a week thereafter (on days -3, 4, 11, and 18). The mice in control groups were intraperitoneally injected with 100 mL distilled water. On days 14- 15, mice in the NK-cell depletion groups and the control groups were euthanized for harvesting of samples. The mice were monitored daily and euthanized when moribund.

*Immunohistochemistry (IHC)*

4 µm mouse melanoma tissue sections were deparaffinized and rehydrated before the citrate buffer antigen retrieval method was performed to unmask the antigenic epitopes. Briefly, slides were arranged in a single layer in a staining holder, submerged in a 500 ml glass beaker with 300 ml of 10 mM citrate buffer at pH 6.0, and incubated at 95-100°C in microwave oven for 10 min. The beaker was then removed from the microwave oven to room temperature and slides were allowed to cool for 1 hour. Next, slides were incubated in 3% hydrogen peroxide for 20 minutes to quench endogenous peroxidase activity. The sections were washed with a solution of phosphate-buffered saline (PBS) and 0.1% Triton three times. They were incubated with 10% normal goat serum in PBS + 0.1% Triton for 30 min to block nonspecific binding sites in the tissue. The tumor sections were incubated with 1:200 (in blocking buffer) rabbit anti-Granzyme B (Abcam, cat#4059) or mouse anti-Ki67 (Cell signaling, Danvers, MA, cat#9499) antibody at 4°C overnight in a wet box in the refrigerator. The secondary antibody used was anti-rabbit AP and anti-mouse HRP antibody (ENZO Biochem, Farmingdale, NY). After staining with the HIGHDEF IHC chromogen substrate DAB and AP (ENZO Biochem), the tissue sections were dehydrated by subsequent alcohol washings using 70%, 95%, and 100% EtOH solutions for 5 minutes each. Total cells were counted under microscope (original magnification, 20x; Carl Zeiss, Thornwood, NY). Cell counts were performed on at least three consecutive slides with three mice in each group.

*Statistical analysis*

All data are represented as a mean with standard error of the mean (SEM). Unpaired two-tailed student's t-tests or one-way ANOVA followed by Tukey multiple comparison test or two-way ANOVA followed by Bonferroni correction when more than two groups were compared (GraphPad Prism, version 6.05, GraphPad Software, Inc.) were used for statistical analysis. P-values less than 0.05 were considered statistically significant.

# Results

*Elevated systemic SIRT2 expression enhances melanoma progression in mice*

The roles of intracellular SIRT2 as either a tumor suppressor or oncogene have been reported in several cancers including liver, breast, brain, and skin melanoma. To determine whether systemic SIRT2

expression plays a role, we examined xenograft melanoma tumor progression in genetic murine models in which SIRT2 was expressed normally in wild-type (WT) mice and overexpressed in transgenic *Sirt2*-knockin (*Sirt2*-KI) mice that contain 3 copies of the *Sirt2* gene [28]. Mice were subcutaneously inoculated with B16-F10 melanoma cells at the connection between the hind limbs and the abdomen, and the tumor growth rate was closely monitored for twenty days before harvesting and measuring the weight and volume of the tumors (Figure 1A). Both WT and *Sirt2*-KI mice had tumor formation rates of 100%; however, *Sirt2*-KI mice developed tumors that were growing significantly faster than those harvested from WT mice. The tumors from *Sirt2*-KI mice weighed more (Figure 1B, $P = 0.0103$) and consistently progressed to a larger volume past 14 days after inoculation (Figure 1C, $P < 0.0001$). Because previous studies have reported intracellular SIRT2 plays a role as a tumor suppressor due to its impact on genomic stability, we used the CRISPR/Cas9 lentivirus and Flag-tagged transfection systems to manipulate SIRT2 expression in B16-F10 melanoma cells to determine whether intracellular SIRT2 status is responsible for the observed tumor growth. B16-F10 cells with vector control (Vehicle), *Sirt2* knockout (*Sirt2*-KO), and *Sirt2* overexpression (*Sirt2-OE)* (Supplemental Figure 1A) were inoculated subcutaneously into wild-type mice using the subcutaneous melanoma model. We observed no difference in their tumor formation, growth rate, and tumor volume over 15 days (Supplemental Figure 1B). With this, we conclude that systemic, rather than intra-tumor, SIRT2 expression positively correlates with murine melanoma tumor progression.

*Increased SIRT2 expression is associated with inhibition of NK cell tumor infiltration and activity within the tumor microenvironment*

To investigate the mechanism of enhanced tumor progression observed with overexpression of systemic SIRT2, we examined whether SIRT2 expression influenced the composition of the tumor microenvironment. Tumors in WT and *Sirt2*-KI mice displayed no significant differences in histology, particularly vascular distribution and quantity of vessels supplying the tumor (data not shown). Because of the integral role the host immune response plays in tumor progression, we examined the tumor infiltration of various immune reactive cells including the T cell, B cell, macrophage, and NK cell. Samples from spleen, blood, and tumor were harvested from our xenograft model and NK cells were distinguished from other leukocytes via flow cytometry by selecting for NKp46 positive and CD3e negative cells [29] (Figure. 2A). No significant findings were observed between immune cell distributions among blood and spleen samples (data not shown). Interestingly, the number of NK cells found within melanoma tumors was significantly decreased in *Sirt2*-KI mice compared to those harvested from WT mice (Figure 2B, $P = 0.0021$). These findings suggest possible involvement of the tumor microenvironment in tumor progression control through SIRT2-mediated inhibition of NK cell infiltration into melanoma tumors.

To further characterize SIRT2 regulation of NK cell activity, immunohistochemistry staining of tumors from *Sirt2*-KI and WT mice was performed to examine the functional and proliferative profiles of NK cells within the tumor microenvironment. Tumoricidal potential was assessed by staining for granzyme B, a cytotoxic mediator produced by NK cells [30,31]. Compared to WT mice, tumors in *Sirt2*-KI mice showed reduced levels of granzyme B (Figure 3A, $P = 0.0486$), suggesting decreased NK cell function. Furthermore, Ki-67 staining revealed significantly decreased NK cell proliferation in *Sirt2*-KI mice (Figure

3B, *P* = 0.0211). These results suggested that systemic SIRT2 promotes tumor progression by inhibiting NK cell tumor infiltration and anti-tumor function.

*SIRT2's effect on melanoma tumor progression is mediated through NK cells*

To examine whether the NK cell is indeed the key immune cell through which SIRT2 affects melanoma growth, we artificially inhibited NK cell function through antibody-mediated NK cell depletion to recreate suppressed NK cell in melanoma TME observed in SIRT2-overexpressing mice. Using anti-AsGM1 antibodies, we depleted the NK cell population within our mouse melanoma xenograft models [32,33]. Consistent with reports from other studies [34-36], antibody-mediated NK cell depletion in WT mice significantly promoted tumor progression as evidenced by a 1.6-fold increase in tumor volume, similar to that of *Sirt2*-KI mice. On the other hand, melanoma tumors grew at a similar rate in *Sirt2*-KI mice, regardless of whether NK cells were depleted (Figure 4, *P* = 0.0038). The significant decrease in tumor progression observed in WT, but not *Sirt2*-KI, mice following NK cell inhibition supports our hypothesis that NK cells are important in SIRT2-mediated tumor progression.

*Pharmacological inhibition of SIRT2 resumes NK cell tumor infiltration and suppresses melanoma progression*

After establishing a relationship between NK cell suppression and SIRT2-mediated melanoma growth, we hypothesized that pharmacological inhibition of SIRT2 function *in vivo* would have a therapeutic effect on tumor progression. SirReal2 *in vivo* inhibition of SIRT2 in mice was confirmed, via Western blot, by measuring the levels of acetylation of K40 (AcK40) on α-tubulin, a classic SIRT2 substrate in the liver (Figure 5A). WT mice were treated with SirReal2 before and after inoculation of B16-F10 melanoma cells, and tumor development was monitored for 19 days. We also included *Sirt2*-KO mouse as genetic control for the specificity of SirReal2-mediated SIRT2 inhibition. As shown in Figure 5B and 5C, SirReal2 treatment significantly slowed tumor progression in WT mice and decreased end tumor volume and weight. It suppressed tumor growth rate and resulted in 2.5-fold smaller tumors by Day 19. However, SIRT2 inhibition had no effect on melanoma tumor growth in *Sirt2*-KO mice. Furthermore, the tumors that developed in *Sirt2*-KO mice had a growth rate and final weight equal to those seen in WT mice treated with SirReal2 (Figure 5B, *P* <0.0001 on Days 17 and 19; Figure 5C, *P* = 0.0002, 0.0001, and 0.0001). To verify the mechanism of tumor suppression, we again identified and quantified infiltrating NK cells distributions of different leukocytes within tumors via flow cytometry analysis. NK cells were distinguished from other leukocytes by selecting for NKp46 positive and CD3e negative cells (Figure 5D). We found that SIRT2 inhibition by SirReal2 resulted in a significant increase of NK cell tumor infiltration compared to the vehicle-treated group in wild-type mice. On the other hand, tumors in *Sirt2*-KO mice demonstrated no change in infiltration by NK cells regardless of SIRT2 inhibition (Figure 5E, *P* = 0.0006). Together, these data illustrate a novel inhibitory role of systemic SIRT2 on NK cell function resulting in tumor progression promotion.

# Discussion

The NAD-dependent histone deacetylase known as SIRT2 shows promise as a therapeutic target in cancer treatment [37]. Its enigmatic role in carcinogenesis is gaining more attention as contradictory studies report it as being either an oncoprotein or a tumor suppressor [38]. Using genetic murine models, we demonstrate that systemic overexpression of SIRT2 promotes melanoma tumor progression through suppression of NK cell tumor infiltration and activity. Antibody-mediated depletion of NK cells increased tumor growth and volume in WT mice, but not *Sirt2*-KI mice, further supporting the integral role of SIRT2. Importantly, pharmacologic inhibition of SIRT2 suppressed tumor progression, identifying a potential therapeutic target.

Currently, the literature supports diverging functions for SIRT2 in tumorigenesis, in a context-dependent manner, that act to modify epigenetic pathways implicated in cancer's initiation, promotion, and progression [38-40]. Our findings illustrate the novel capacity of SIRT2 to enhance subcutaneous melanoma progression while raising the vital question of at what point does SIRT2, a protein that promotes genomic integrity in healthy cells, transition into what can only be described as a cancer promoter. The data compiled from this study reveals a potential mechanism explaining SIRT2's impact upon tumor progression based on suppression of NK cell function within the tumor microenvironment. We acknowledge that our findings further add to SIRT2's controversial role considering SIRT2 has been reported to promote the cytotoxic effects of NK cells in hepatocellular carcinoma; however, these studies differ in the types of tumors studied and the approach to SIRT2 expression manipulation. The inherent differences in hepatocellular carcinoma and melanoma could have substantial impacts on tumor progression, just as we have seen in studies looking at breast cancer and glioblastoma [8,10]. Furthermore, the effect of SIRT2 expression on NK cell tumoricidal activity was investigated using SIRT2 knockdown within liver NK cells, a strategy that results in genetics vastly different from the *Sirt2*-KI mice used in our model. Combined with previously published studies, this could support a dual role for SIRT2 as illustrated in Figure 6. SIRT2 could act as a tumor suppressor during initiation through DNA repair and genomic stability while promoting progression of established tumors through NK cell suppression.

Our results identify NK cells as a key player in SIRT2-mediated tumor progression, suggesting that tumors generated in *Sirt2*-KI mice develop more aggressively due to a deficiency of NK cells infiltrating in TME. In addition, once the reduced number of NK cells invade the tumor, they exhibit decreased cytotoxic activity and proliferation. SIRT2's impact on NK cells within the tumor microenvironment invokes the need for additional studies examining SIRT2's effects on other NK cell processes such as maturation, migration, and cytotoxic properties as these issues are not currently characterized. Understanding these connections is crucial as emerging data describes NK cells as a key constituent in immunotherapy response and resistance [24]. Interestingly, NK cells were recently shown to increase the abundance of stimulatory dendritic cells within the microenvironment of human melanoma, which enhanced cytotoxic T cell function required for anti-PD-1 immunotherapy [41]. Perhaps SIRT2 expression could act as a predicter of immunotherapy response and provide a target to reverse treatment resistance and non-response through NK cells. Considering up to 80% of patients do not respond or develop resistance to immunotherapy, elucidating targets to overcome these outcomes is imperative.

In summary, this work suggests a novel relationship between systemic SIRT2 expression, NK cell behavior in the tumor microenvironment, and melanoma tumor progression. This novel role of systemic SIRT2 may be relevant to the progression of carcinomas of other organs and might help explain the conflicting data describing SIRT2's role in tumorigenesis. With further study of the relationship between SIRT2, NK cells, and tumor progression, a new target for the challenges of immunotherapy could be developed.

# Declarations


### Acknowledgements

We gratefully acknowledge Dr. David Sinclair (Harvard Medical School) for providing essential reagents. This study was supported by NIH grants R01 CA188500 to F.X. and A.C. and R01 CA163838 to F.X.


### Author Contributions

F.X., M.Z., and J.Y. conceived and designed the experiments. M.Z., W.D., J.G., M.P., and H.Y. performed the experiments. F.X., M.Z., W.D., and S.A. analyzed the data. S.A., J.G., M.Z., J.Y. and F.X. wrote the manuscript. All authors reviewed and approved the manuscript for publication.

### Additional Information

### Competing interests

The authors declare no competing interests.

# References


1. Chang, H.C. & Guarente, L. SIRT1 and other sirtuins in metabolism. *Trends Endocrinol Metab* **25**, 138-45 (2014).
2. Mendes, K.L., Lelis, D.F. & Santos, S.H.S. Nuclear sirtuins and inflammatory signaling pathways. *Cytokine Growth Factor Rev* **38**, 98-105 (2017).
3. Guarente, L. Sirtuins in aging and disease. *Cold Spring Harb Symp Quant Biol* **72**, 483-8 (2007).
4. Lagunas-Rangel, F.A. Current role of mammalian sirtuins in DNA repair. *DNA Repair (Amst)* **80**, 85-92 (2019).
5. Inoue, T., Hiratsuka, M., Osaki, M. & Oshimura, M. The molecular biology of mammalian SIRT proteins: SIRT2 in cell cycle regulation. *Cell Cycle* **6**, 1011-8 (2007).
6. Kim, H.S. et al. SIRT2 maintains genome integrity and suppresses tumorigenesis through regulating APC/C activity. *Cancer Cell* **20**, 487-99 (2011).
7. Chen, M. et al. Sirtuin2 enhances the tumoricidal function of liver natural killer cells in a mouse hepatocellular carcinoma model. *Cancer Immunol Immunother* **68**, 961-971 (2019).

8. Shi, P., Zhou, M. & Yang, Y. Upregulated tumor sirtuin 2 expression correlates with reduced TNM stage and better overall survival in surgical breast cancer patients. *Ir J Med Sci* **189**, 83-89 (2020).
9. Park, S.H. et al. SIRT2 is a tumor suppressor that connects aging, acetylome, cell cycle signaling, and carcinogenesis. *Transl Cancer Res* **1**, 15-21 (2012).
10. Funato, K. et al. SIRT2-mediated inactivation of p73 is required for glioblastoma tumorigenicity. *EMBO Rep* **19**(2018).
11. Wilking-Busch, M.J., Ndiaye, M.A., Huang, W. & Ahmad, N. Expression profile of SIRT2 in human melanoma and implications for sirtuin-based chemotherapy. *Cell Cycle* **16**, 574-577 (2017).
12. Wang, Y., Yu, L., Ding, J. & Chen, Y. Iron Metabolism in Cancer. *Int J Mol Sci* **20**(2018).
13. Yang, X. et al. Sirtuin 2 regulates cellular iron homeostasis via deacetylation of transcription factor NRF2. *J Clin Invest* **127**, 1505-1516 (2017).
14. Heinonen, T. et al. Dual Deletion of the Sirtuins SIRT2 and SIRT3 Impacts on Metabolism and Inflammatory Responses of Macrophages and Protects From Endotoxemia. *Front Immunol* **10**, 2713 (2019).
15. Xu, L. et al. The SIRT2/cMYC Pathway Inhibits Peroxidation-Related Apoptosis In Cholangiocarcinoma Through Metabolic Reprogramming. *Neoplasia* **21**, 429-441 (2019).
16. DeNardo, D.G. et al. CD4(+) T cells regulate pulmonary metastasis of mammary carcinomas by enhancing protumor properties of macrophages. *Cancer Cell* **16**, 91-102 (2009).
17. Binnewies, M. et al. Understanding the tumor immune microenvironment (TIME) for effective therapy. *Nat Med* **24**, 541-550 (2018).
18. Santolla, M.F. & Maggiolini, M. The FGF/FGFR System in Breast Cancer: Oncogenic Features and Therapeutic Perspectives. *Cancers (Basel)* **12**(2020).
19. Unoki, M. & Nakamura, Y. Growth-suppressive effects of BPOZ and EGR2, two genes involved in the PTEN signaling pathway. *Oncogene* **20**, 4457-65 (2001).
20. Trimboli, A.J. et al. Pten in stromal fibroblasts suppresses mammary epithelial tumours. *Nature* **461**, 1084-91 (2009).
21. O'Sullivan, T. et al. Interleukin-17D mediates tumor rejection through recruitment of natural killer cells. *Cell Rep* **7**, 989-98 (2014).
22. Ruscetti, M. et al. NK cell-mediated cytotoxicity contributes to tumor control by a cytostatic drug combination. *Science* **362**, 1416-1422 (2018).
23. Urbonas, V. et al. Natural killer cell-based immunotherapy: a new fighter against melanoma? *Melanoma Res* **29**, 208-211 (2019).
24. Huntington, N.D., Cursons, J. & Rautela, J. The cancer-natural killer cell immunity cycle. *Nat Rev Cancer* **20**, 437-454 (2020).
25. Saddawi-Konefka, R. et al. Nrf2 Induces IL-17D to Mediate Tumor and Virus Surveillance. *Cell Rep* **16**, 2348-58 (2016).

26. Cao, W. et al. SIRT2 mediates NADH-induced increases in Nrf2, GCL, and glutathione by modulating Akt phosphorylation in PC12 cells. *FEBS Lett* **590**, 2241-55 (2016).
27. Serrano, L. et al. The tumor suppressor SirT2 regulates cell cycle progression and genome stability by modulating the mitotic deposition of H4K20 methylation. *Genes Dev* **27**, 639-53 (2013).
28. North, B.J. et al. SIRT2 induces the checkpoint kinase BubR1 to increase lifespan. *EMBO J* **33**, 1438-53 (2014).
29. Dong, W. et al. The Mechanism of Anti-PD-L1 Antibody Efficacy against PD-L1-Negative Tumors Identifies NK Cells Expressing PD-L1 as a Cytolytic Effector. *Cancer Discov* **9**, 1422-1437 (2019).
30. Chollat-Namy, M. et al. The pharmalogical reactivation of p53 function improves breast tumor cell lysis by granzyme B and NK cells through induction of autophagy. *Cell Death Dis* **10**, 695 (2019).
31. Oberoi, P., Jabulowsky, R.A., Bahr-Mahmud, H. & Wels, W.S. EGFR-targeted granzyme B expressed in NK cells enhances natural cytotoxicity and mediates specific killing of tumor cells. *PLoS One* **8**, e61267 (2013).
32. Alvarez-Breckenridge, C.A. et al. NK cells impede glioblastoma virotherapy through NKp30 and NKp46 natural cytotoxicity receptors. *Nat Med* **18**, 1827-34 (2012).
33. Han, J. et al. TGFbeta Treatment Enhances Glioblastoma Virotherapy by Inhibiting the Innate Immune Response. *Cancer Res* **75**, 5273-82 (2015).
34. Gao, Y. et al. Tumor immunoevasion by the conversion of effector NK cells into type 1 innate lymphoid cells. *Nat Immunol* **18**, 1004-1015 (2017).
35. Zhang, Q. et al. Blockade of the checkpoint receptor TIGIT prevents NK cell exhaustion and elicits potent anti-tumor immunity. *Nat Immunol* **19**, 723-732 (2018).
36. Zhang, Z. et al. Gasdermin E suppresses tumour growth by activating anti-tumour immunity. *Nature* **579**, 415-420 (2020).
37. Karwaciak, I. et al. SIRT2 Contributes to the Resistance of Melanoma Cells to the Multikinase Inhibitor Dasatinib. *Cancers (Basel)* **11**(2019).
38. Carafa, V., Altucci, L. & Nebbioso, A. Dual Tumor Suppressor and Tumor Promoter Action of Sirtuins in Determining Malignant Phenotype. *Front Pharmacol* **10**, 38 (2019).
39. Bosch-Presegue, L. & Vaquero, A. The dual role of sirtuins in cancer. *Genes Cancer* **2**, 648-62 (2011).
40. Zhang, L., Kim, S. & Ren, X. The Clinical Significance of SIRT2 in Malignancies: A Tumor Suppressor or an Oncogene? *Front Oncol* **10**, 1721 (2020).
41. Barry, K.C. et al. A natural killer-dendritic cell axis defines checkpoint therapy-responsive tumor microenvironments. *Nat Med* **24**, 1178-1191 (2018).
42. Zhang, M., Du, W., Acklin, S., Jin, S. & Xia, F. SIRT2 protects peripheral neurons from cisplatin-induced injury by enhancing nucleotide excision repair. *J Clin Invest* **130**, 2953-2965 (2020).

# Figures

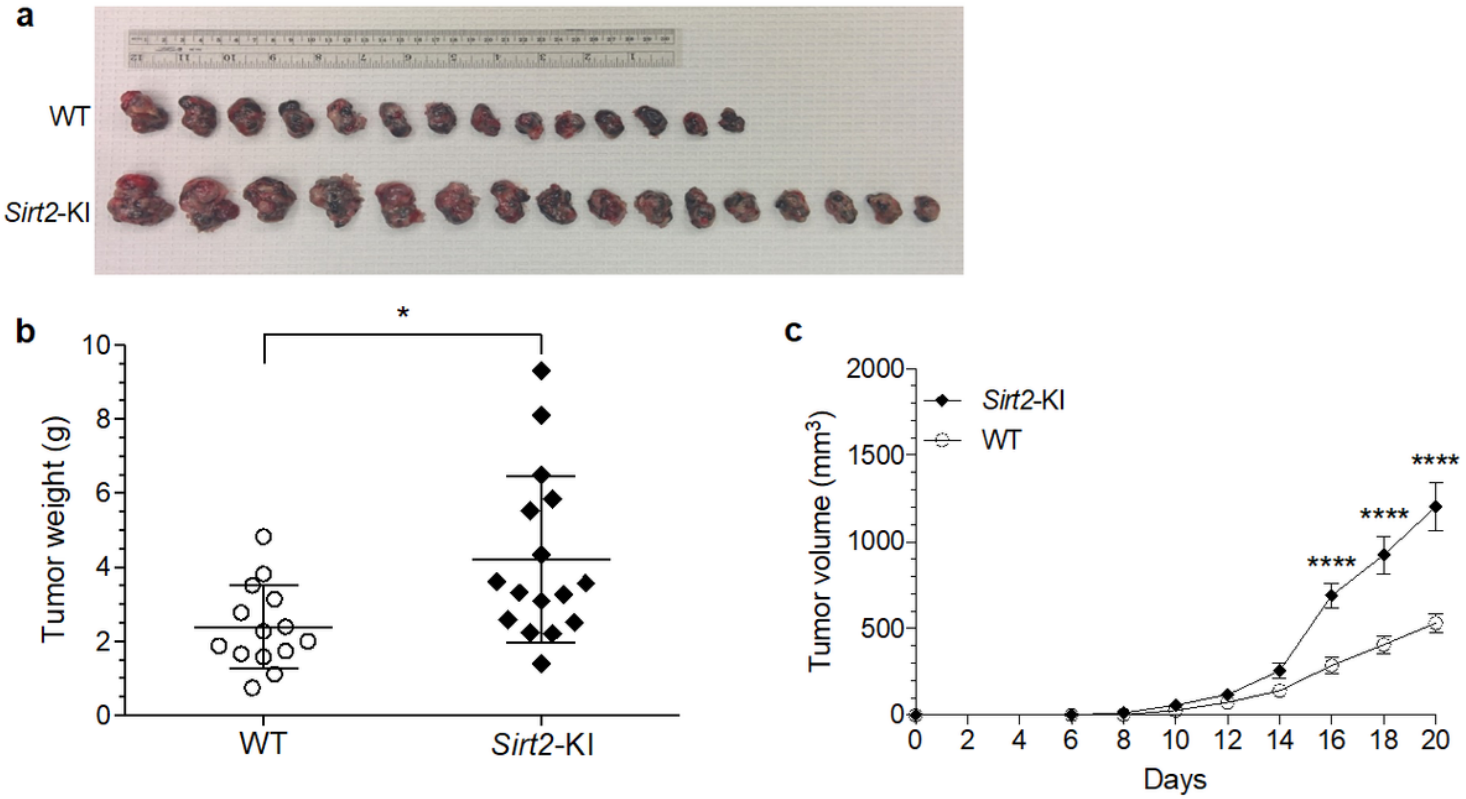


## Figure 1

SIRT2 overexpression increases growth of melanoma tumors in mice (A) Gross specimens of subcutaneous melanoma tumors harvested from Sirt2-KI and WT mice inoculated with 1 x 105 B16-F10 melanoma cells. (B) Tumors in WT (n = 14) and Sirt2-KI (n = 16) mice were harvested on Day 20 and weighed. Student's t-test. (C) Tumor progression and size were monitored 20 days post injection in WT and Sirt2-KI mice (n = 3). Two-way ANOVA with Bonferroni correction. Data points are mean values ± SEM.*p<0.05 and ****p<0.0001.

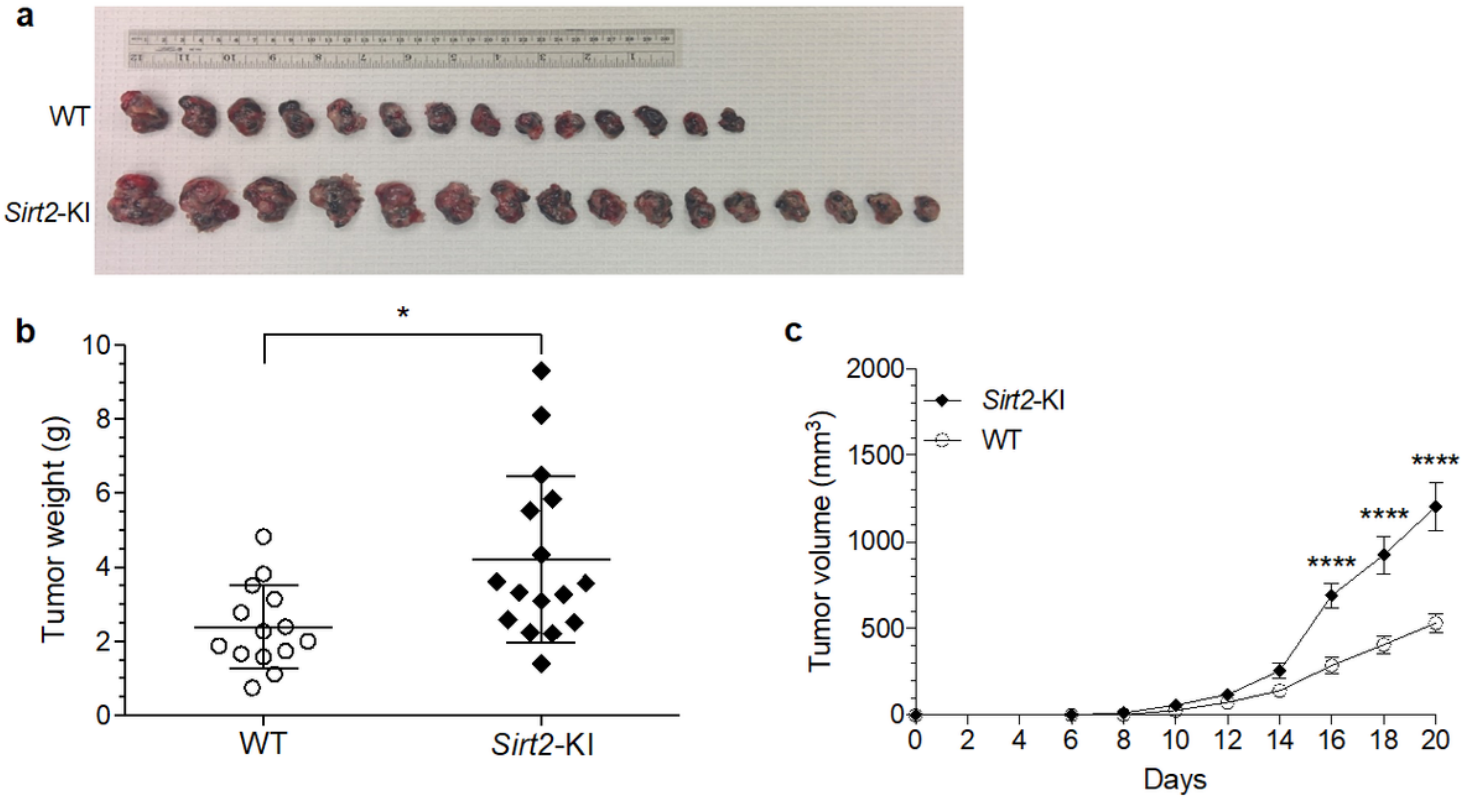


## Figure 1

SIRT2 overexpression increases growth of melanoma tumors in mice (A) Gross specimens of subcutaneous melanoma tumors harvested from Sirt2-KI and WT mice inoculated with 1 x 105 B16-F10 melanoma cells. (B) Tumors in WT (n = 14) and Sirt2-KI (n = 16) mice were harvested on Day 20 and weighed. Student's t-test. (C) Tumor progression and size were monitored 20 days post injection in WT and Sirt2-KI mice (n = 3). Two-way ANOVA with Bonferroni correction. Data points are mean values ± SEM.*p<0.05 and ****p<0.0001.

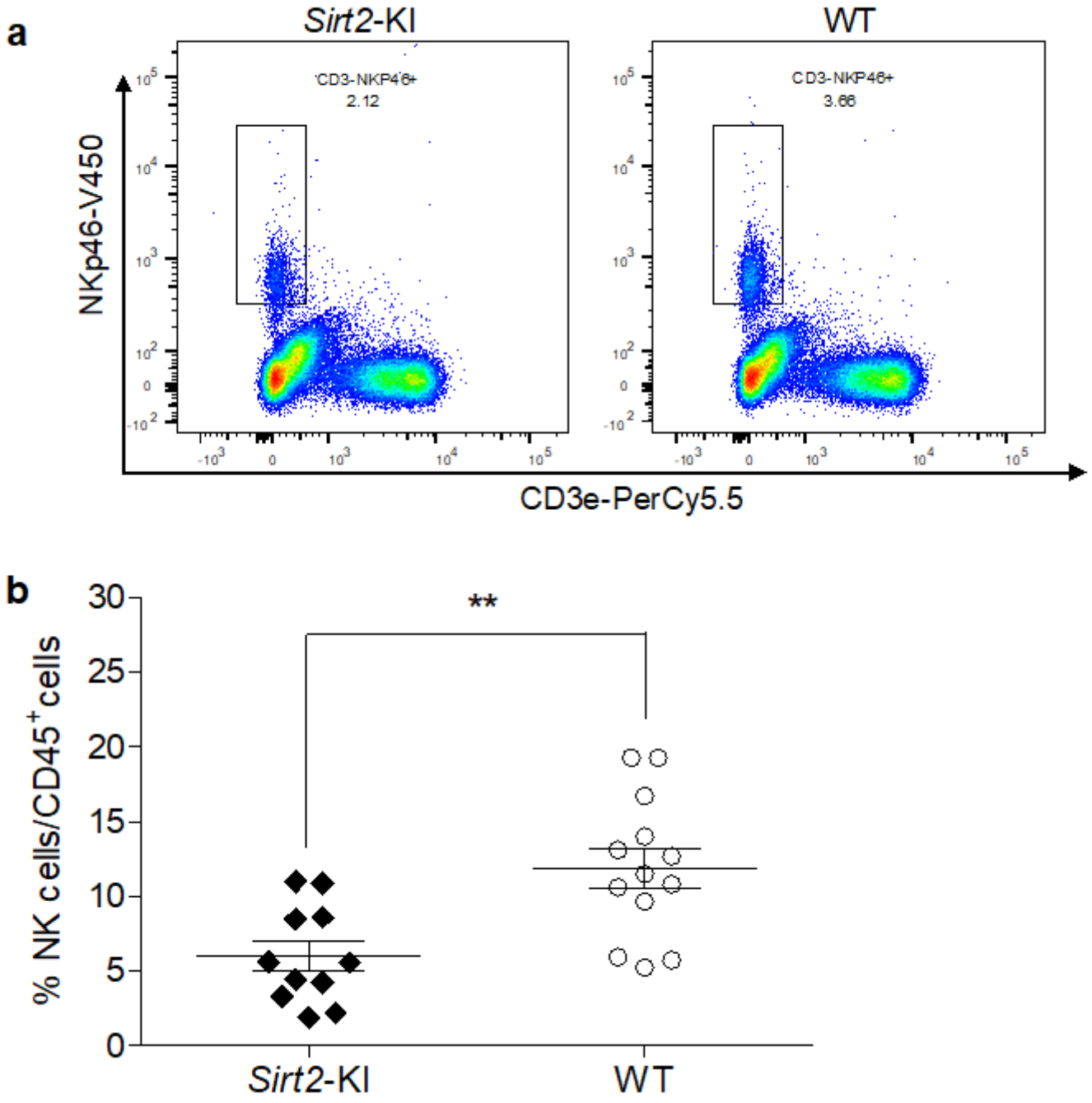


## Figure 2

Natural killer cell distribution is altered by SIRT2 expression (A) Subcutaneous melanoma tumors from WT and Sirt2-KI mice were harvested and analyzed by flow cytometry for the prevalence of NK cells among leukocytes. The gating strategy was designed to isolate NK cells by selecting for cells that are NKp46 positive and CD3e negative. (B) The percentage of tumor-infiltrating leukocytes that expressed the NK cell signature were quantified in WT and Sirt2-KI mice. Columns represent mean values with error bars representing the SEM. n = 11, 13. Student's t-test,**p<0.01.

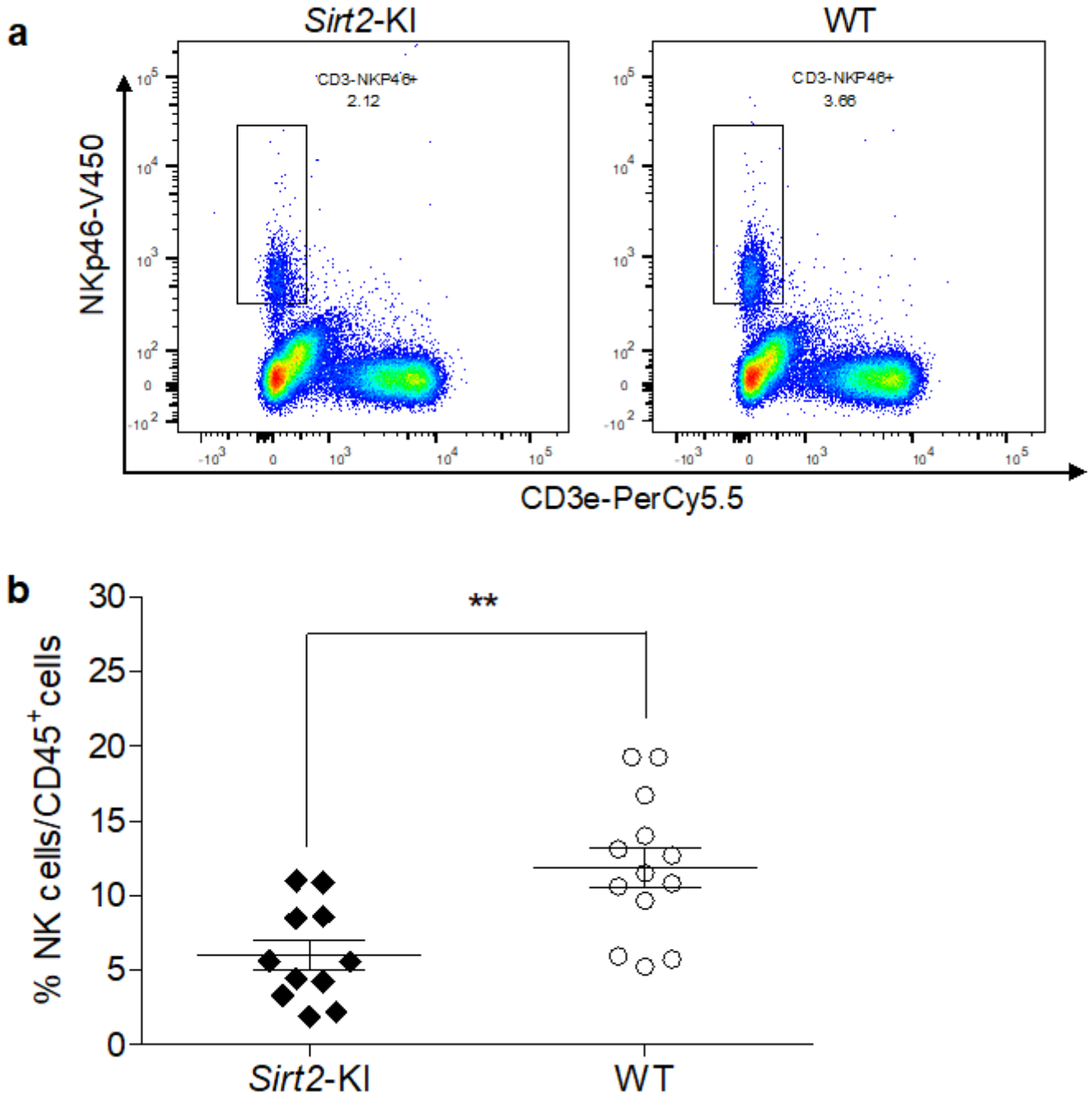


## Figure 2

Natural killer cell distribution is altered by SIRT2 expression (A) Subcutaneous melanoma tumors from WT and Sirt2-KI mice were harvested and analyzed by flow cytometry for the prevalence of NK cells among leukocytes. The gating strategy was designed to isolate NK cells by selecting for cells that are NKp46 positive and CD3e negative. (B) The percentage of tumor-infiltrating leukocytes that expressed the NK cell signature were quantified in WT and Sirt2-KI mice. Columns represent mean values with error bars representing the SEM. n = 11, 13. Student's t-test,**p<0.01.

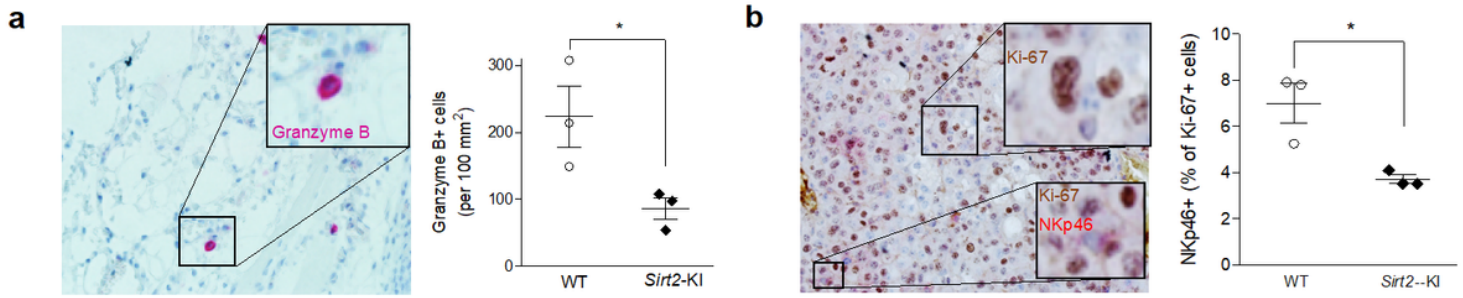


## Figure 3

NK cell function is decreased in SIRT2-overexpressing mice Immunohistochemical staining of subcutaneous melanoma samples from 3 Sirt2-KI and 3 WT mice was used to determine tumor-infiltrating NK cell functional activity and proliferation. Images represent staining in WT mice. (A) The number of granzyme B positive cells per 100 mm2 is representative of functional NK cell activation within the tumor area. (B) Cells stained positive for NKp46 were categorized as NK cells and are represented by one of three sections. Quantitative analysis is representative of 5 fields from each sample where the number of NKp46 cells divided by the total Ki-67 number to yield a percentage. Samples that expressed both the Ki-67 proliferative marker and the NK signature represent healthy NK cell proliferation. Data points represent mean values and error bars designate SEM; n = 3, Student's t-test, *p<0.05.

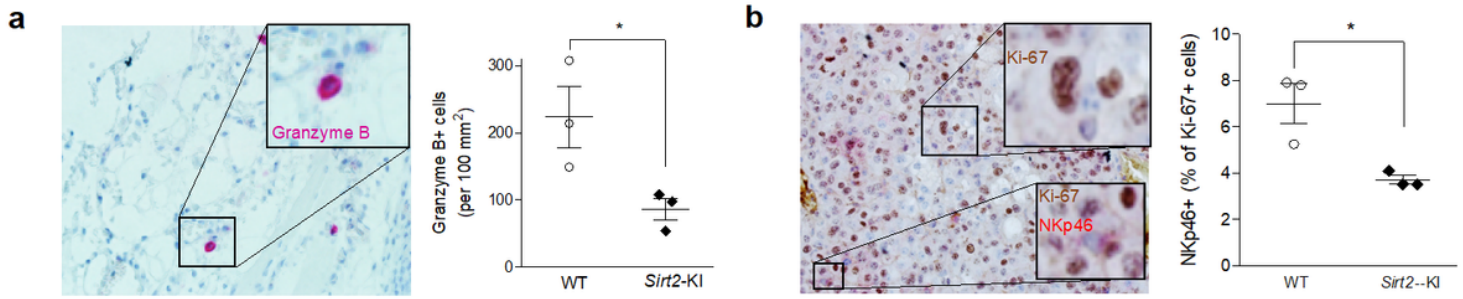


## Figure 3

NK cell function is decreased in SIRT2-overexpressing mice Immunohistochemical staining of subcutaneous melanoma samples from 3 Sirt2-KI and 3 WT mice was used to determine tumor-infiltrating NK cell functional activity and proliferation. Images represent staining in WT mice. (A) The number of granzyme B positive cells per 100 mm2 is representative of functional NK cell activation within the tumor area. (B) Cells stained positive for NKp46 were categorized as NK cells and are represented by one of three sections. Quantitative analysis is representative of 5 fields from each sample where the number of NKp46 cells divided by the total Ki-67 number to yield a percentage. Samples that expressed both the Ki-67 proliferative marker and the NK signature represent healthy NK cell proliferation. Data points represent mean values and error bars designate SEM; n = 3, Student's t-test, *p<0.05.

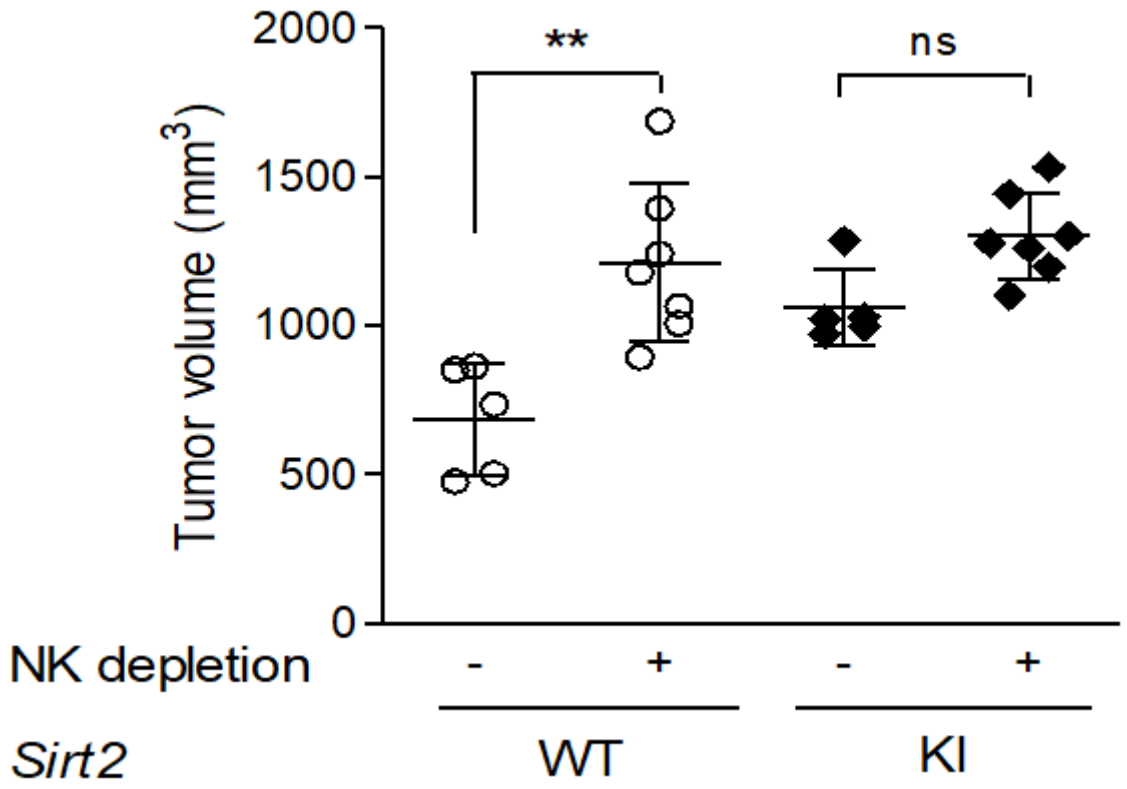


**Figure 4**

The effect of SIRT2 on tumor progression is mediated through NK cells WT (n = 6 and 5) and Sirt2-KI (n = 7 and 5) mice were divided into two groups with one receiving anti-AsGM1 to deplete NK cell populations, and the other was treated with saline. Following inoculation with B16-F10 melanoma cells, tumors were monitored for growth and harvested after 21 days. Data points represent mean values ± SEM. One-way ANOVA with post-hoc Tukey HSD test, **p < 0.01.

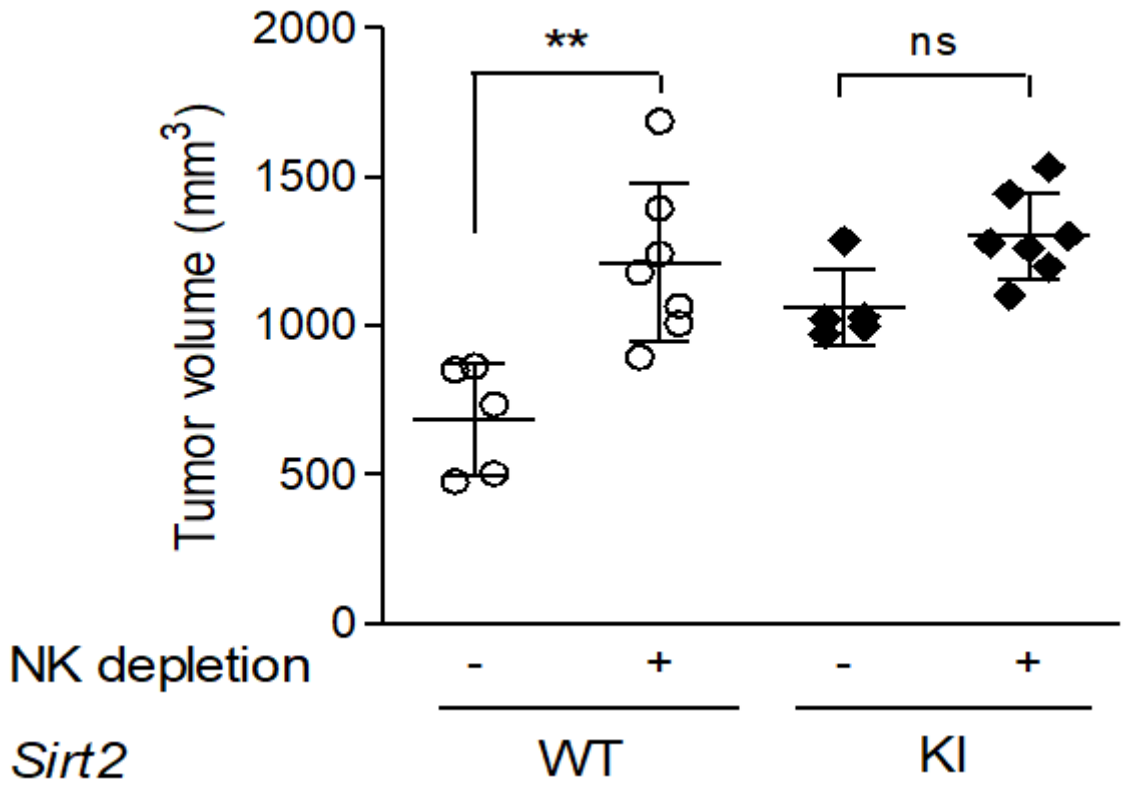


**Figure 4**

The effect of SIRT2 on tumor progression is mediated through NK cells WT (n = 6 and 5) and Sirt2-KI (n = 7 and 5) mice were divided into two groups with one receiving anti-AsGM1 to deplete NK cell populations, and the other was treated with saline. Following inoculation with B16-F10 melanoma cells, tumors were monitored for growth and harvested after 21 days. Data points represent mean values ± SEM. One-way ANOVA with post-hoc Tukey HSD test, **p < 0.01.

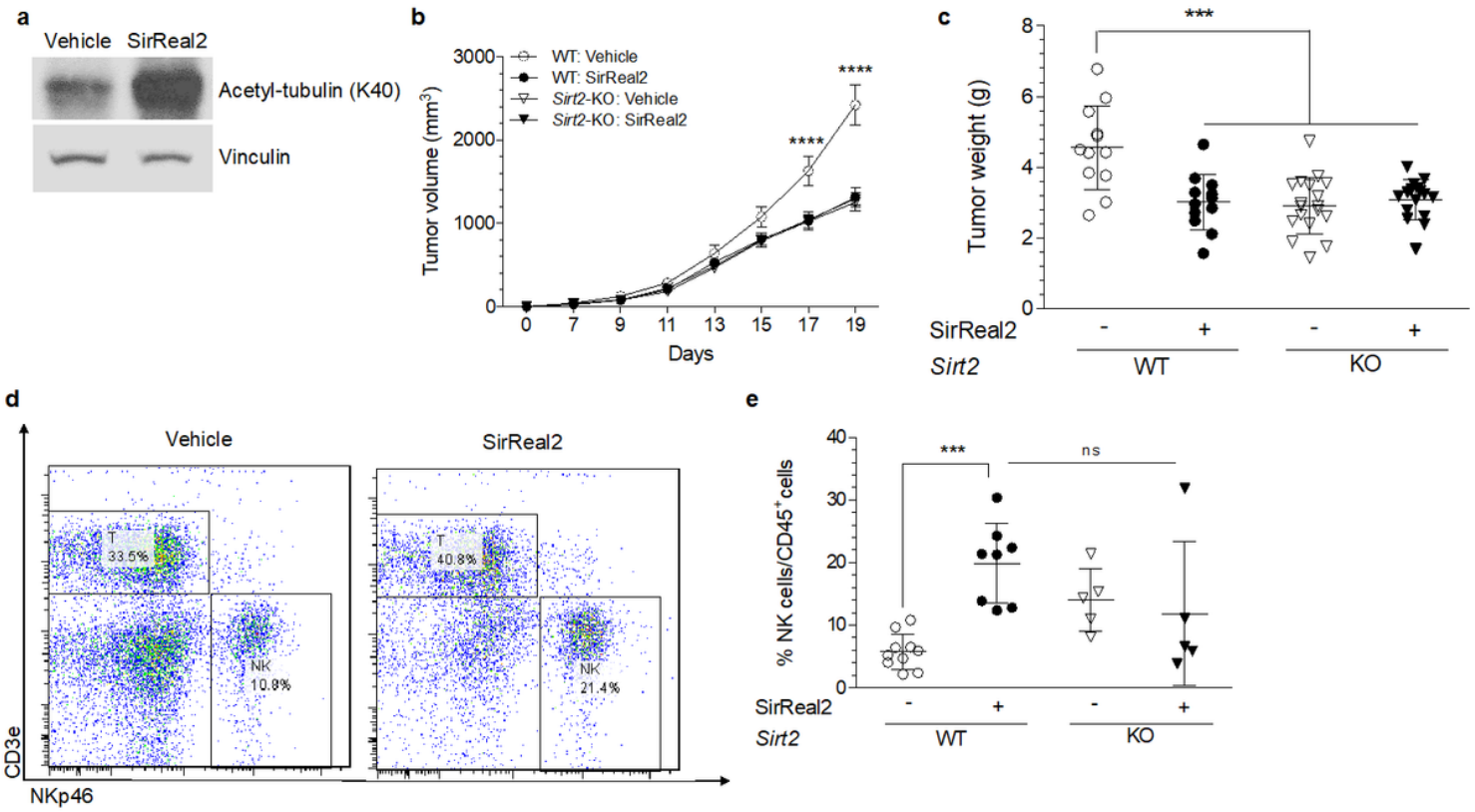


## Figure 5

Pharmacological inhibition of SIRT2 enhances NK cell function and suppresses tumor progression (A) Western blot showing decreased SIRT2 expression and deacetylase activity, as indicated by increased levels of α-tubulin K40 acetylation, in C57BL/6 mice treated with SirReal2, a small molecule SIRT2 inhibitor (n=3). (B) Tumor progression and size were monitored up to 19 days following injection of B16-F10 cells into WT and Sirt2-KO mice treated with SirReal2 or vehicle (n = 12 and 18 for WT and Sirt2-KO). Two-way ANOVA with Bonferroni correction. (C) Tumors were harvested on Day 19 and weighed. (D) Subcutaneous melanoma tumors from WT mice were harvested and analyzed by flow cytometry for the prevalence of NK cells among leukocytes. The gating strategy was designed to identify NK cells as cells that are NKp46 positive and CD3e negative. (E) Abundance of NK cells as a percent of total leukocytes infiltrating melanoma tumors in WT (n = 10 and 8) and Sirt2-KO (n = 5) mice treated with vehicle or SirReal2 was quantified. (C,E) One-way ANOVA with post-hoc Tukey HSD. Data points are mean values ± SEM. ***p<0.001 and ****p<0.0001.

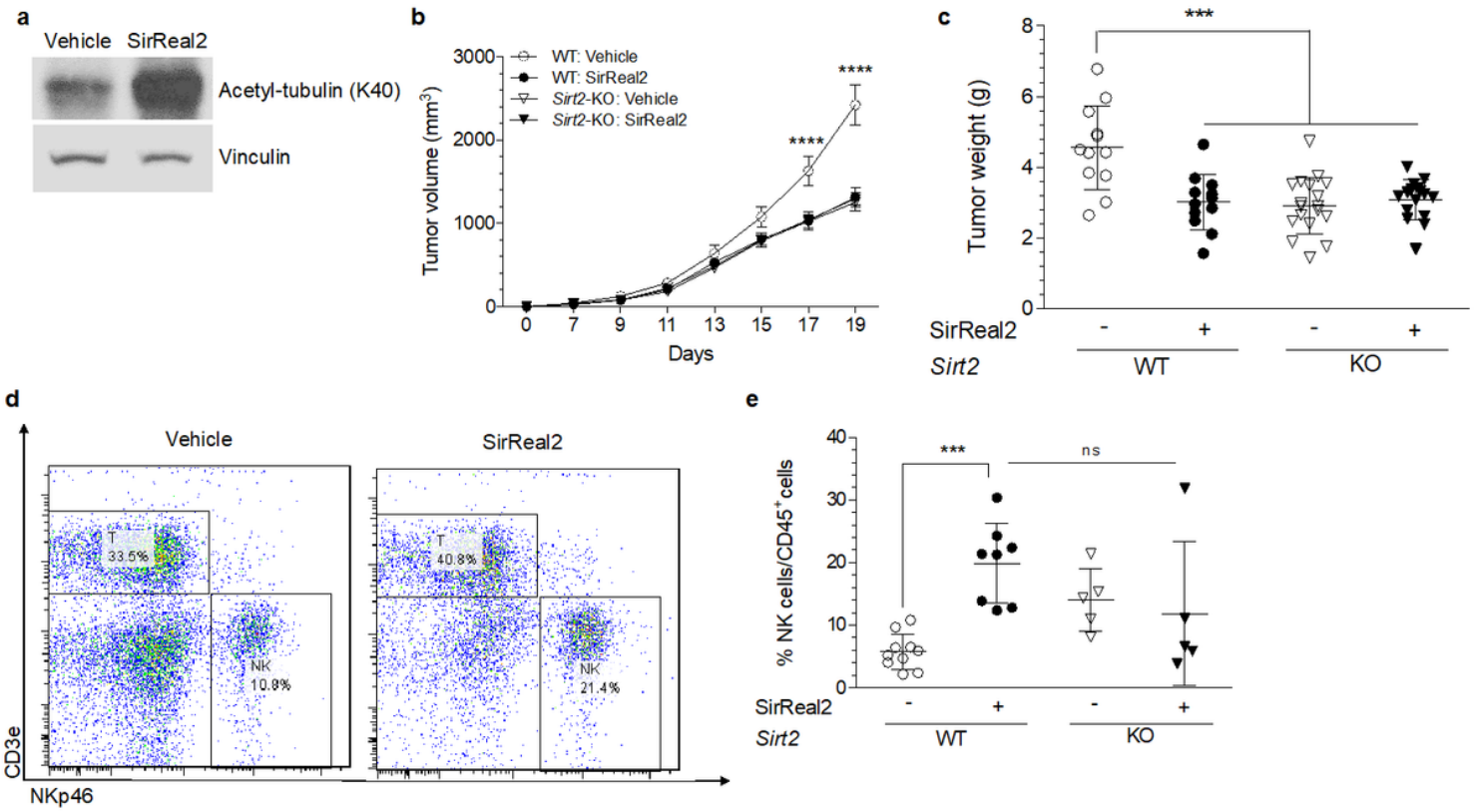


## Figure 5

Pharmacological inhibition of SIRT2 enhances NK cell function and suppresses tumor progression (A) Western blot showing decreased SIRT2 expression and deacetylase activity, as indicated by increased levels of α-tubulin K40 acetylation, in C57BL/6 mice treated with SirReal2, a small molecule SIRT2 inhibitor (n=3). (B) Tumor progression and size were monitored up to 19 days following injection of B16-F10 cells into WT and Sirt2-KO mice treated with SirReal2 or vehicle (n = 12 and 18 for WT and Sirt2-KO). Two-way ANOVA with Bonferroni correction. (C) Tumors were harvested on Day 19 and weighed. (D) Subcutaneous melanoma tumors from WT mice were harvested and analyzed by flow cytometry for the prevalence of NK cells among leukocytes. The gating strategy was designed to identify NK cells as cells that are NKp46 positive and CD3e negative. (E) Abundance of NK cells as a percent of total leukocytes infiltrating melanoma tumors in WT (n = 10 and 8) and Sirt2-KO (n = 5) mice treated with vehicle or SirReal2 was quantified. (C,E) One-way ANOVA with post-hoc Tukey HSD. Data points are mean values ± SEM. ***p<0.001 and ****p<0.0001.

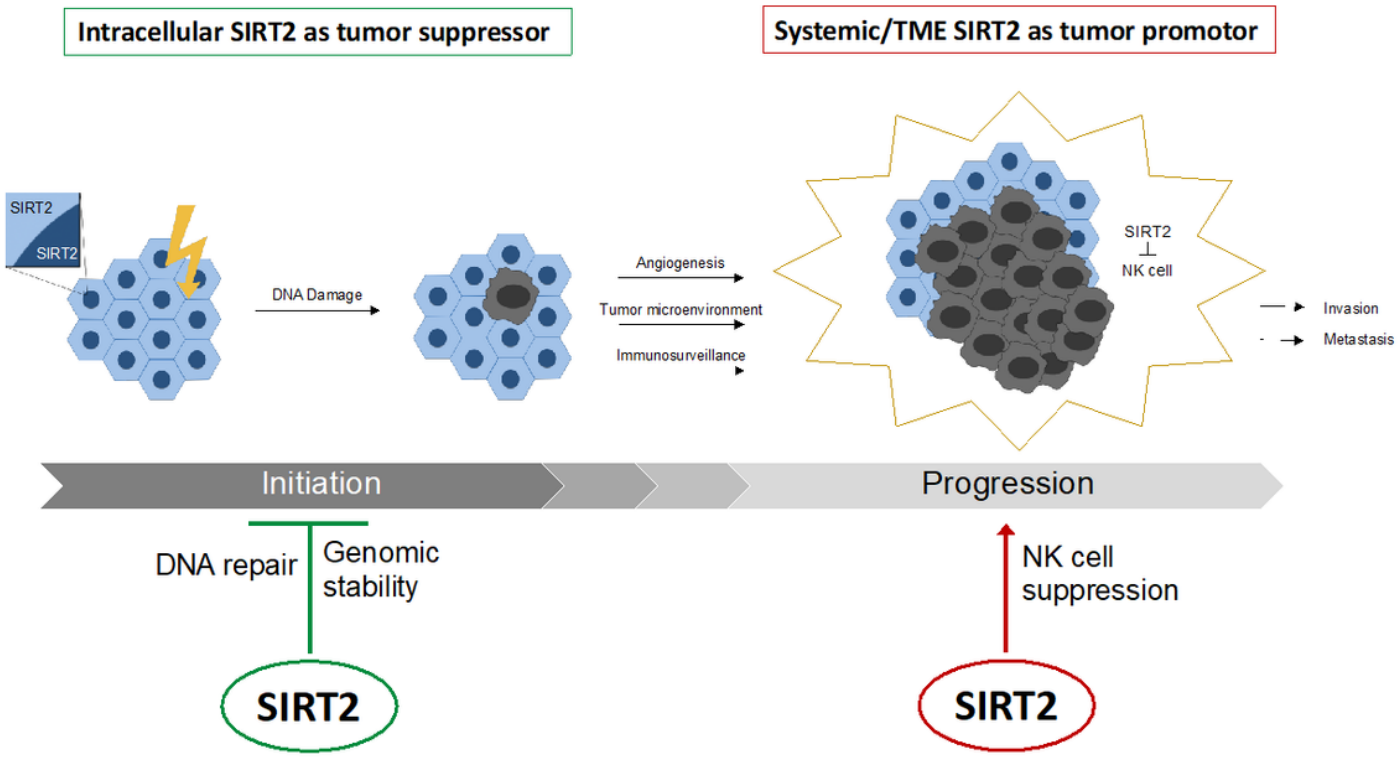


## Figure 6

The dual role of SIRT2 in cancer initiation and progression An illustration of SIRT2's potential roles in cancer initiation and progression are shown with treatment strategies targeting SIRT2 proposed.

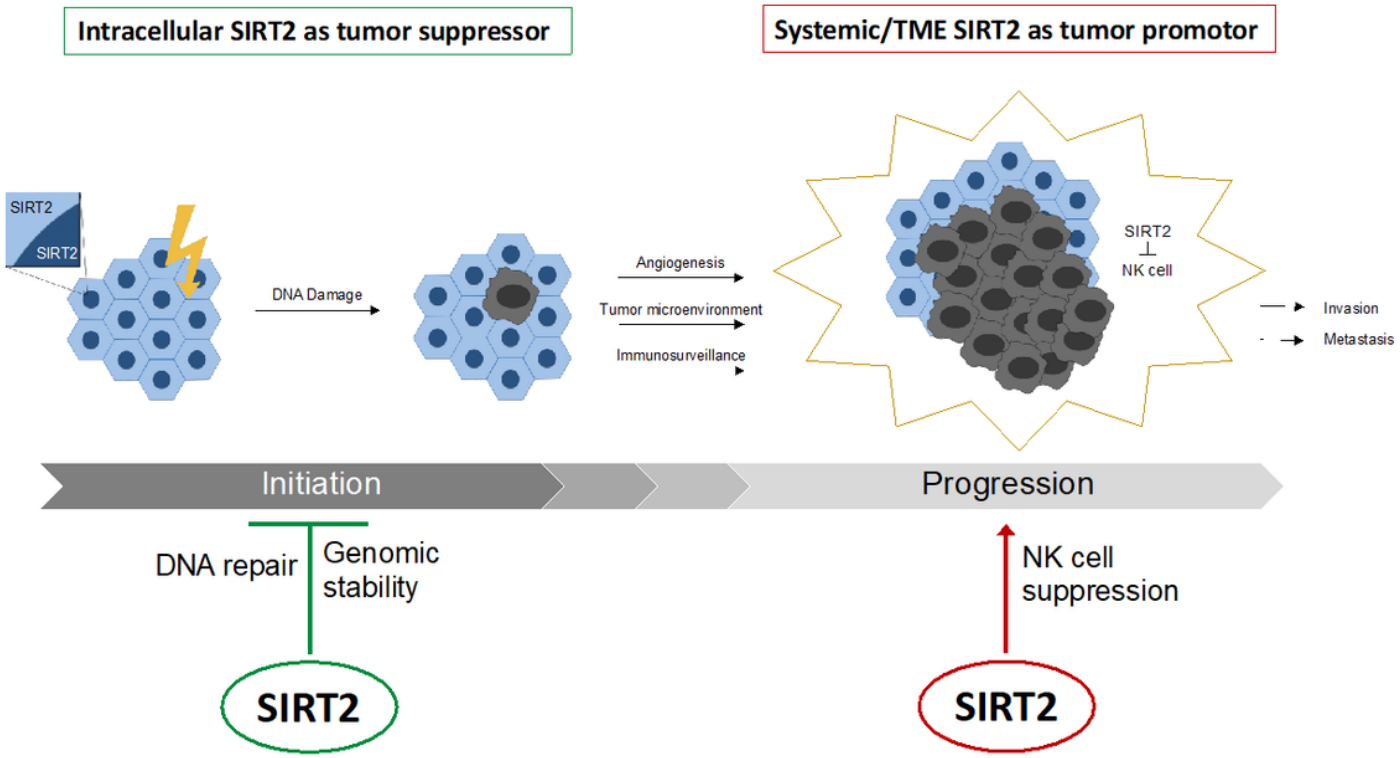

**Figure 6**

The dual role of SIRT2 in cancer initiation and progression An illustration of SIRT2's potential roles in cancer initiation and progression are shown with treatment strategies targeting SIRT2 proposed.

## Supplementary Files

This is a list of supplementary files associated with this preprint. Click to download.

- SIRT2NKCellSupplementalFinal.pdf
- SIRT2NKCellSupplementalFinal.pdf